

# INVESTIGATING LUNAR SURFACE MATURITY WITH MULTIPLE DATA METHODS AND WAVELENGTHS

A. C. Martin<sup>1</sup>, A. M. Stickle<sup>1</sup>, J. T. S. Cahill<sup>1</sup>, J. A. Grier<sup>2</sup>, B. Greenhagen<sup>1</sup>, G. W. Patterson<sup>1</sup>,  
<sup>1</sup>Johns Hopkins University Applied Physics Laboratory, Laurel, MD, 20723, USA (anna.martin@jhuapl.edu), <sup>2</sup>Planetary Science Institute, Tucson AZ USA.

**Introduction:** Understanding surface evolution of the Moon is essential for understanding surface processes and determining relative ages between features. The lunar surface, when exposed to the space environment, goes through a modification process called “maturation” [1]. The physical properties of the regolith changes with time and these changes can be characterized using different maturity indices (i.e. Optical maturity OMAT) [2]. The evolution of the regolith is thought to occur through multiple processes. One key process is the build up of agglutinate or glass content [1, 3-9]. Multiple studies show that agglutinates account for large portions of mature soils [1, 5, 10, 11]. The amount of sub-microscopic iron (SMFe), trapped solar wind nitrogen [10], and solar wind sputtering and vapor deposition [12, 13] in the material can have contributing factors as well. Sampling maturity effects from different processes indicates that this evolution can be tracked across wavelengths [11].

**Preliminary Methods:** In a preliminary comparison [14], three craters: Byrgius A, Dufay B, and Golitsyn J were surveyed using different maturity methods to look for correlations of maturity as a function of wavelength. The methods for representing those maturities were OMAT, Lunar Reconnaissance Orbiter Camera (LROC), Diviner, and Miniature Radio Frequency (Mini-RF). After reviewing these three craters, the conclusion was that maturity can be tracked across wavelengths but a more detailed comparison is necessary.

For this abstract, we will build on that previous work by evaluating 36 craters using the same methodology. The craters are drawn from the Lunar Impact Crater Database [15] and they were chosen based on morphology and whether Mini-RF coverage was available. The goal is to better understand if maturity trends can be correlated because they manifest differently at different wavelengths. If the initial conclusion holds true, this can provide a powerful insight into surface evolution on the Moon.

**Data Comparisons:** OMAT comes from extracting optical maturity parameters from multispectral data (here, we use data from Clementine and the Kaguya Multi-band Imager). Using these parameters, overall maturity can be characterized on lunar soils and crater ejecta [2]. Grier et al. [2] used OMAT to classify Byrgius A as *young*, Dufay B as *intermediate*, and Golitsyn J as *old* based on profiles of OMAT across the ejecta blankets (Figure 1).

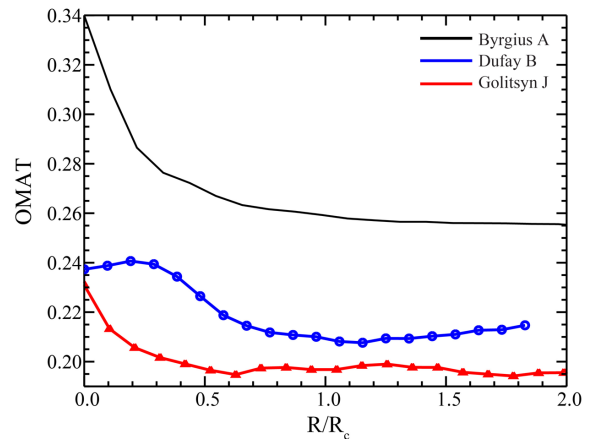


Figure 1. OMAT values for the preliminary craters. Youngest crater ejecta shows a higher OMAT value. Intermediate crater ejecta is lower, while the oldest crater shows the lowest OMAT value.

**LROC:** Data from the LROC wide angle camera (WAC) gives us a near-global seven band mosaic (321-689 nm), where we can investigate the lunar surface at ultraviolet wavelengths. The findings from Denevi et al [16], suggested that UV reflectance data is key for quantifying maturation of young soils. Our study is using an RGB image to examine maturation at given craters;  $R = 415$  nm,  $G = 321/415$  nm ratio, and  $B = 321/360$  nm ratio. When viewing the RGB image, green indicates the most mature, pink indicates low  $321/415$  nm ratio, and yellow indicates high  $321/415$  nm ratio. We can see a distinction in these RGB images for the 3 preliminary craters and expect to see the same trend in this study (Figure 2).

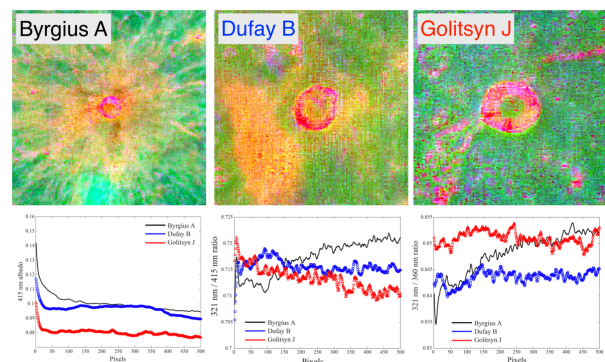


Figure 2. (Top) The 3 craters shown as RGB images from UV WAC data. (Bottom) The 3 bands corresponding to the RGB image plotted against pixels: 415nm, 321/415nm, 321/360nm.

**Mini-RF:** Mini-RF is a dual-polarized synthetic aperture radar that acquired data at two wavelengths, S-band (12.6 cm) and X-band (4.2 cm). The Circular Polarization Ratio (CPR) is used to represent surface roughness at radar wavelength [17, 18]. Younger ejecta blankets contain more blocky materials which can cause increased backscatter from the radar signal at the lunar surface. This will result in a higher CPR value than a return from a smoother surface. As craters age, those blocky materials start to weather and break down, thus resulting in less back-scattered signal, which causes a decrease in the returned radar power (Figure 3). The Mini-RF data can also be evaluated using an  $m\text{-}\chi$  decomposition, which provides information about the scattering characteristics of the surface [19, 20] and which can be visualized using RGB color-coded images. As the radar wave interacts with the surface, it can be scattered off of various reflectors with a single or double bounce or through the surface with volume scattering. Younger surfaces with blocky materials typically result in higher double bounce signal, while older surfaces experience increased volume scattering.

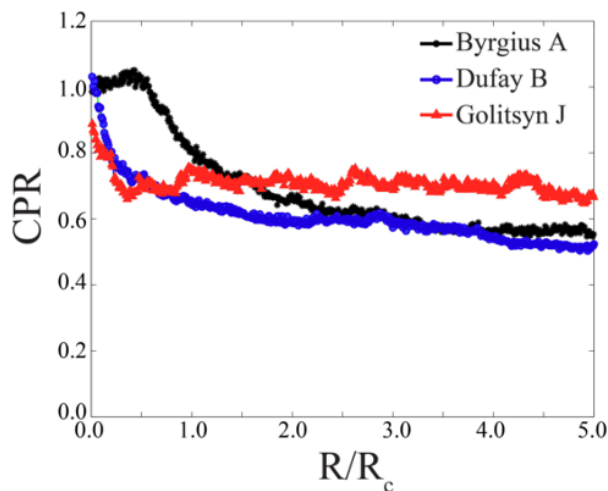


Figure 3. The CPR values for the youngest crater are the highest/most easily observed over the ejecta blanket. The other craters show the maturing surface can depend on age.

**Diviner:** Using the rock abundance parameter from Diviner, we can observe degradation of surface rocks [21]. A lack of rocks in an area suggests a more mature surface, which gets validated when looking at the nighttime surface temperature. With maturation, both rock abundance and nighttime temperature decreases (figure 4). Another indicator for maturity from Diviner data is the Christensen Feature (CF) that can compositionally indicate silicate mineralogy [22]. Increasing maturity means longer wavelengths, which holds true in our preliminary study.

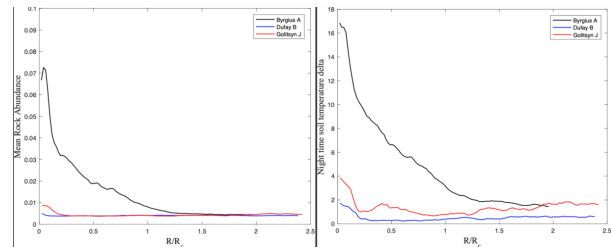


Figure 4. Mean rock abundance (left) and nighttime soil temperature (right) from Diviner data. Byrgius A, the youngest crater, shows evidence for the most rocks (high RA and high nighttime soil temperature), while Dufay B and Golitsyn J are a little trickier to distinguish, but each exhibit evidence of less rocky ejecta blankets.

**Methods and Future Work:** To compare all 36 craters, the data need to be processed and analyzed uniformly. Because we are interested in ejecta blankets, we started with creating “postage stamps” of each crater. To create profiles of all the craters and their given data methods, code was developed in IDL to generate user-defined profiles across ejecta blankets. Average radial profiles can be defined over the complete 360° circle or a user-defined azimuth range. If gaps are present within longitudinal data, the profile will only average over areas containing that data.

Because we are using multiple datasets to understand how maturity indicators manifest across wavelength, it is important to examine each dataset individually and as a whole. By utilizing multiple datasets at multiple wavelengths, we hope to provide a more comprehensive understanding of maturation and degradation of craters on the lunar surface.

**References:** [1] McKay, D.S., et al. (1974) *Proc. Lunar. Sci. Conf* 5<sup>th</sup>, p. 887-906; [2] Grier et al. (2001) *J. Geophys. Res.* 106(E12), 32847-32862; [3] Adams, J.B. and T.B. McCord (1971) *Science*, 171, 567-571; [4] Adams, J.B., and M.P. Charette (1975) *The Moon*, 13, 293-299; [5] Charette, M.P., et al. (1976) *Proc. Lunar Sci. Conf.* 7<sup>th</sup>, p. 2579-2592; [6] Wells, E., and B. Hapke (1977) *Science*, 195, 977-979; [7] Pieters, C. M. et al (1993) *J. Geophys. Res. Planet.* 98(E11), 20817-20824; [8] Britt, D.T., and C.M. Pieters (1994) *Geochim. Cosmochim. Acta* 58, 3905-3919; [9] Lucey, P. G., & Riner, M. A. (2011) *Icarus*, 212(2), 451-462; [10] Charette, M.P., and J.B. Adams (1975), *Proc. Lunar Sci. Conf.* 6<sup>th</sup>, 2281-2289; [11] Gold, T., et al. (1976) *Proc. Lunar Sci. Conf.* 7<sup>th</sup>, p. 901-911; [12] Hapke, B., et al (1975) *Moon*, 13, 339-354; [13] Lucey, P.G., et al. (2000) *J. Geophys. Res.*, 105, 20,377-20,386; [14] Stickle, A.M., et al (2016) *Lunar and Planetary Science Conference*, 47<sup>th</sup>, 2928; [15] Losiak, A.T., (2009) *Lunar Impact Crater Database*, revised LPI (2011); [16] Denevi, B. et al. (2014) *J. Geophys. Res. Planet.* 119, 976-997; [17] Campbell et al. (2010), *Icarus*, 208, 565-573; [18] Carter et al. (2012), *JGR*, 117, E00H09; [19] Raney, R. K. et al. (2011), *Proc. of the IEEE*, 99, 808-823; [20] Carter et al. (2012), *JGR*, 117, E00H09; [21] Bandfield, J.L., et al. (2011) *J. Geophys. Res.*, 116, E00H02; [22] Greenhagen, B. T., et al. (2010) *Science*, 329, 1507-150.